

Adaptive Tube MPC: Beyond a Common Quadratically Stabilizing Feedback Gain [★]

Anchita Dey, Shubhendu Bhasin

Electrical Engineering Department, Indian Institute of Technology Delhi, Hauz Khas, New Delhi, Delhi 110016, India

Abstract

This paper proposes an adaptive tube framework for model predictive control (MPC) of discrete-time linear time-invariant systems subject to parametric uncertainty and additive disturbances. In contrast to conventional tube-based MPC schemes that employ fixed tube geometry and constraint tightening designed for worst-case uncertainty, the proposed approach incorporates online parameter learning to progressively refine the parametric uncertainty set and update the parameter estimates. These updates are used to adapt the components of the MPC optimization problem, including the prediction model, feedback gain, terminal set, and tube cross-sections. As the uncertainty set contracts, the required amount of constraint tightening reduces and the tube shrinks accordingly, yielding less conservative control actions. Recursive feasibility, robust constraint satisfaction, and closed-loop stability are formally established. Furthermore, the framework does not require the existence of a common quadratically stabilizing linear feedback gain for the entire parametric uncertainty set, thereby relaxing a standard assumption in existing tube-based MPC formulations. Numerical examples illustrate the effectiveness of the proposed approach.

Key words: Model predictive control, Adaptive control, Control of constrained systems, Optimization under uncertainties.

1 Introduction

Model predictive control (MPC) is an optimization-based control strategy that uses a system model to predict future system behavior and computes an optimal sequence of control inputs by minimizing a cost function of predicted states and inputs, subject to hard constraints. In the standard MPC formulation, the constrained optimal control problem (COCP) relies on an accurate model of the system dynamics for state prediction [17]. In the presence of modeling errors or disturbances, however, the true system evolution may deviate from the predicted trajectories, potentially leading to constraint violations and loss of recursive feasibility or stability. Since exact model knowledge is rarely available in practice, the problem of designing MPC schemes for systems affected by parametric uncertainty and additive disturbances has received considerable attention in the literature.

Robust MPC methods are mostly based on either min-max optimization or tube-based approaches and have

been extensively studied in the literature. These methods are typically designed for systems with known parameters subject to unknown additive disturbances [4, 20, 27], or for systems with parametric uncertainty, with or without additive disturbances [3, 10, 16]. In the latter case, however, the uncertain parameters are typically treated as unknown but fixed, and no mechanism is employed to learn or refine their estimates online. To reduce conservatism and improve performance, adaptive MPC schemes have recently been proposed [9, 13, 19, 21, 23], where the system parameters, the sets containing them, or both are updated using online data, while prediction errors are handled through robust tubes.

Among robust MPC formulations, homothetic tube MPC [20, 27] provides a convenient parametrized structure for bounding prediction errors and formulating the COCP. Consequently, recent research has focused on reducing the conservatism associated with fixed tube constructions. For instance, [22] proposes a flexible tube structure based on zonotopes, where the parameters defining the tube cross-sections are optimized online. The framework in [18] considers systems with additive disturbances only and constructs tubes through an online-optimized blending of offline-computed invariant sets corresponding to different stabilizing feedback gains. Self-tuning tubes are proposed in [30] for sys-

[★] Corresponding author A. Dey.

Email addresses: anchitadey.ee.india@gmail.com (Anchita Dey), sbhasin@ee.iitd.ac.in (Shubhendu Bhasin).

tems with both parametric uncertainty and additive disturbances.

For systems with parametric uncertainty and constraints imposed on all states, most existing approaches [3, 7–9, 13, 19, 21–23, 30] assume the existence of a common quadratically stabilizing linear state feedback gain for the entire uncertainty set [14]. Specifically, it is assumed that there exists a common linear feedback gain that stabilizes the origin of a linear time-invariant (LTI) system whose state and input matrices correspond to any element of the parametric uncertainty set. This assumption, however, significantly restricts the class of admissible uncertainty sets [1, 11]. In general, a parametric uncertainty set may not admit quadratic stabilization, and even when quadratic stability can be established, a linear feedback gain that stabilizes every element of the set may not exist [25]. Even in cases where such a common stabilizing gain exists, the construction of a common terminal set satisfying the state and input constraints for all admissible systems may still be infeasible or highly conservative, further restricting the practical applicability of such approaches.

Data-driven predictive control frameworks [2, 5] provide an alternative that avoids the need for a common stabilizing feedback gain. However, since these methods rely on an offline-constructed Hankel matrix derived from previously collected data, their performance may degrade if the system dynamics changes during online operation.

In this work, we propose the notion of *adaptive tubes* for MPC of discrete-time LTI systems subject to both parametric uncertainty and additive disturbances. Specifically, we construct homothetic tubes whose cross-sectional geometry is updated online based on the evolving parameter point estimate and the refined parametric uncertainty set. The resulting adaptive tube framework avoids the common but restrictive assumption of the existence of a single quadratically stabilizing linear feedback gain for the entire uncertainty set [3, 7–9, 13, 19, 21–23, 30], thereby reducing conservatism.

To achieve this, the system matrices are decomposed into an estimated component and an unknown component, with the latter treated as part of a lumped additive disturbance. This representation enables the formulation of a tube-based COCP with a structure similar to that of standard homothetic tube MPC [20, 27], while yielding improved constraint tightening through the use of separate forward reachable disturbance sets [4] rather than a single worst-case disturbance bound. The available state and input data are used to update both the parametric uncertainty set [15] and the parameter point estimate through a projection-modified normalized gradient descent law [12]. The resulting reduction in parametric

uncertainty leads to online recomputation of the tightened constraints, the tube cross-sectional shape, and the terminal set. Furthermore, the terminal ingredients are constructed using a feedback gain associated with the current parameter estimate rather than requiring a common gain for all elements of the uncertainty set. Although this adaptation modifies the underlying COCP and may affect feasibility, recursive feasibility is ensured by a backup formulation invoked when necessary. The proposed scheme also guarantees robust exponential stability [24, Def. 2] and boundedness of all signals.

The main contributions of this work are twofold. First, we introduce the notion of adaptive tubes for MPC of discrete-time LTI systems with parametric uncertainty and additive disturbances, where the tube cross-sections, terminal set and constraint tightening are updated online based on parameter learning and uncertainty set contraction. Second, the proposed framework avoids the commonly imposed assumption of the existence of a quadratically stabilizing linear feedback gain for the entire parametric uncertainty set by constructing terminal ingredients using the current parameter estimate. Further, we establish recursive feasibility, robust exponential stability of the origin, and boundedness of all closed-loop signals for the resulting adaptive tube MPC scheme.

Notations: For two sets $\mathbb{A}, \mathbb{B} \subseteq \mathbb{R}^n$, the Minkowski sum $\mathbb{A} \oplus \mathbb{B} \triangleq \{a + b \mid a \in \mathbb{A}, b \in \mathbb{B}\}$ and $a \oplus \mathbb{B} \triangleq \{a + b \mid b \in \mathbb{B}\}$, where $a \in \mathbb{R}^n$, the Pontryagin difference $\mathbb{A} \ominus \mathbb{B} \triangleq \{a \mid a + b \in \mathbb{A} \forall b \in \mathbb{B}\}$, the set multiplication $\mathbb{A}\mathbb{B} \triangleq \{ab \mid a \in \mathbb{A}, b \in \mathbb{B}\}$, where a, b are of conformal dimensions. The convex hull of all elements in \mathbb{B} is denoted by $\text{co}(\mathbb{B})$. The notation $W \succ 0$ ($\succeq 0$) implies the matrix W is symmetric positive-definite (positive semi-definite). $\|\cdot\|_\infty$, $\|\cdot\|_2$ and $\|\cdot\|_F$ denote ∞ -norm, 2-norm and Frobenius norm, respectively, and $\|b\|_W^2 \triangleq b^\top W b$ for a vector b . The notation $a_{i|t}$ represents the value of a at time $t + i$ predicted at time t , and $(\cdot)^*$ on any term denotes its optimal value. A sequence $\{c(p), c(p + 1), \dots, c(q - 1), c(q)\}$ is represented as $\{c(i)\}_{i=p:q}$, and the set of all integers from a to b by \mathbb{I}_a^b . Any signal belonging to \mathcal{L}_∞ implies it is bounded. A sequence vector z_t is said to belong to $\mathcal{S}(m)$ if $\sum_{i=t}^{t+k} z_i^\top z_i \leq c_0 m k + c_1 \forall t \in \mathbb{I}_1^\infty$, a given constant $m \geq 0$, and some $k \in \mathbb{I}_1^\infty$, where $c_0, c_1 \geq 0$ [12, Theorem 4.11.2].

2 Problem Statement

Consider the constrained discrete-time LTI system subject to external disturbance

$$\begin{aligned} x_{t+1} &= Ax_t + Bu_t + d_t, & (1) \\ x_t &\in \mathbb{X}, u_t \in \mathbb{U} \quad \forall t \in \mathbb{I}_0^\infty, & (2) \end{aligned}$$

where $x_t \in \mathbb{R}^n$, $u_t \in \mathbb{R}^m$, and $d_t \in \mathbb{R}^n$ denote the state, input, and external disturbance, respectively, at time t . The disturbance d_t and the system parameter $\psi \triangleq \begin{bmatrix} A & B \end{bmatrix} \in \mathbb{R}^{n \times (n+m)}$ are unknown but belong to sets \mathbb{D} and Ψ , respectively. The sets \mathbb{X} , \mathbb{U} and \mathbb{D} are known convex polytopes containing their origins in their respective interiors. The set $\Psi \subseteq \mathbb{R}^{n \times (n+m)}$ is the convex hull of known vertices $\psi^{[1]}, \psi^{[2]}, \dots, \psi^{[L]}$, where L is a known finite positive integer. Further, for each $\hat{\psi} \triangleq \begin{bmatrix} \hat{A} & \hat{B} \end{bmatrix} \in \Psi$, \exists a pair (P, K) specific to $\hat{\psi}$ such that $P \succ 0$, and

$$P - (\hat{A} + \hat{B}K)^\top P (\hat{A} + \hat{B}K) - Q - K^\top R K \succeq 0, \quad (3)$$

for some given matrices $Q, R \succ 0$, where $P, Q \in \mathbb{R}^{n \times n}$, $R \in \mathbb{R}^{m \times m}$ and $K \in \mathbb{R}^{m \times n}$. This condition implies that each system corresponding to $\hat{\psi} \in \Psi$ is stabilizable and admits a stabilizing linear feedback gain K with a quadratic Lyapunov function $x^\top P x$, which is a standard assumption in MPC design [17, 20, 27].

The *objective* is to design a suitable control u_t that drives the state of the system (1) to its origin while ensuring that the hard constraints (2) are satisfied despite the presence of the disturbance d_t . For the known dynamics (A and B are known) and disturbance-free case, classical approaches [17] could be used to solve the COCP P1 in a receding horizon fashion.

$$\text{P1:} \quad \min_{\mu_t} \sum_{i=0}^{N-1} (\|x_{i|t}\|_Q^2 + \|u_{i|t}\|_R^2) + \|x_{N|t}\|_P^2$$

subject to $x_{0|t} = x_t$, $x_{i+1|t} = Ax_{i|t} + Bu_{i|t} \forall i \in \mathbb{I}_0^{N-1}$,
 $x_{i|t} \in \mathbb{X}$, $u_{i|t} \in \mathbb{U} \forall i \in \mathbb{I}_0^{N-1}$, $x_{N|t} \in \mathbb{X}_{TS} \subseteq \mathbb{X}$,

where $\mu_t \triangleq \{u_{i|t}\}_{i=0:N-1}$, and \mathbb{X}_{TS} is the terminal set (refer to [17, Ch. 2] for details).

The classical COCP P1 is not directly solvable in the presence of uncertainties in A , B and d_t , and therefore requires reformulation. In the subsequent sections, motivated by set membership-based identification [15, 21, 23, 29] and homothetic tube-based MPC methods [20, 27], we reformulate the COCP using an adaptive tube framework that is designed to reduce the uncertainty in ψ at each time instant.

Due to hard constraints on the system's states and inputs, the adaptive tube framework is equipped with a robust fallback mechanism to ensure constraint satisfaction regardless of parameter learning. The robust tube-based method serves as a backup if adaptation renders the modified COCP infeasible. We therefore start by developing the robust framework.

3 COCP components without adaptation

A major motivation for this work is to relax the requirement of a common quadratically stabilizing linear feedback gain for the parametric uncertainty set Ψ , a common assumption in tube-based MPC frameworks for systems with uncertain parameters (see [3, 7–9, 13, 19, 21–23, 30]). To this end, we rewrite the system dynamics in (1) as follows.

$$x_{t+1} = \hat{A}_t x_t + \hat{B}_t u_t + \underbrace{(A - \hat{A}_t)x_t + (B - \hat{B}_t)u_t}_{=: w_t} + d_t, \quad (4)$$

where the parameters \hat{A}_t, \hat{B}_t are the estimates of A, B obtained at time t using a subsequently designed adaptive law and $\begin{bmatrix} \hat{A}_t & \hat{B}_t \end{bmatrix}$ belong to the updated set Ψ_t . The term w_t acts as a lumped additive disturbance. In the absence of parameter adaptation, $\hat{A}_t = \hat{A}_0, \hat{B}_t = \hat{B}_0$ and $\Psi_t = \Psi_0 \forall t \in \mathbb{I}_0^\infty$, where $\Psi_0 \triangleq \Psi$. Throughout this section, we use the suffix t for easy extension to the adaptive case.

3.1 Disturbance set characterization

The knowledge of $\mathbb{X}, \mathbb{U}, \mathbb{D}, \Psi_t$ along with \hat{A}_t and \hat{B}_t is used to characterize the set \mathbb{W}_t containing every possible value of $w_t \forall t \in \mathbb{I}_0^\infty$. Define

$$\Phi_t \triangleq \left\{ \xi \in \mathbb{R}^{n \times (n+m)} \mid \xi + \begin{bmatrix} \hat{A}_t & \hat{B}_t \end{bmatrix} \in \Psi_t \right\}, \quad (5a)$$

$$\Phi_{A_t} \triangleq \left\{ \xi \in \mathbb{R}^{n \times n} \mid \begin{bmatrix} \xi & \eta \end{bmatrix} \in \Phi_t, \eta \in \mathbb{R}^{n \times m} \right\}, \quad (5b)$$

$$\Phi_{B_t} \triangleq \left\{ \xi \in \mathbb{R}^{n \times m} \mid \begin{bmatrix} \eta & \xi \end{bmatrix} \in \Phi_t, \eta \in \mathbb{R}^{n \times n} \right\}. \quad (5c)$$

Using definitions (5b) and (5c), the set \mathbb{W}_t is given by

$$\mathbb{W}_t \triangleq \Phi_{A_t} \mathbb{X} \oplus \Phi_{B_t} \mathbb{U} \oplus \mathbb{D}. \quad (6)$$

A less conservative characterization of the sets containing w_t is obtained by leveraging forward reachable sets of the state x_t in the subsequent N steps¹. At time t , the state measurement x_t is used to compute the sets for $x_{t+1}, x_{t+2}, x_{t+3}, \dots, x_{t+N}$ by propagating the dynamics (1). Since the sets for $x_{t+i} \forall i \in \mathbb{I}_1^N$ depend on the current state x_t , we denote these as $\mathbb{X}_{i,t}$ where i is the number of forward steps ahead of the current time t . The sets are constructed recursively as follows.

$$\mathbb{X}_{0,t} \triangleq \{x_t\}, \quad (7a)$$

$$\mathbb{X}_{i+1,t} \triangleq (\Psi_{A_t} \mathbb{X}_{i,t} \oplus \Psi_{B_t} \mathbb{U} \oplus \mathbb{D}) \cap \mathbb{X}, \quad (7b)$$

¹ We focus on only N steps since the sets for w_t are used in constraint tightening for the homothetic tube in a COCP with a prediction horizon N .

where

$$\Psi_{A_t} \triangleq \left\{ \xi \in \mathbb{R}^{n \times n} \mid \begin{bmatrix} \xi & \eta \end{bmatrix} \in \Psi_t, \eta \in \mathbb{R}^{n \times m} \right\}, \quad (8a)$$

$$\Psi_{B_t} \triangleq \left\{ \xi \in \mathbb{R}^{n \times m} \mid \begin{bmatrix} \eta & \xi \end{bmatrix} \in \Psi_t, \eta \in \mathbb{R}^{n \times n} \right\}. \quad (8b)$$

We only require $\mathbb{X}_{i,t} \forall i \in \mathbb{I}_0^{N-1}$. Using (5a)-(5c), (7a)-(8b), the sets containing w_{t+i} are given by

$$\mathbb{W}_{i,t} \triangleq \Phi_{A_t} \mathbb{X}_{i,t} \oplus \Phi_{B_t} \mathbb{U} \oplus \mathbb{D} \quad \forall i \in \mathbb{I}_0^{N-1}, \quad (9)$$

which are used to make robust state predictions in the MPC COCP.

3.2 Terminal set construction

Without adaptation, $\mathbb{W}_t \equiv \mathbb{W}_0$ and $\mathbb{W}_{i,t} \equiv \mathbb{W}_{i,0}$. While $\mathbb{W}_{i,t}$ contains the possible values of $w_{t+i} \forall i \in \mathbb{I}_0^{N-1}$ starting at any given t , the set \mathbb{W}_t is a superset of $\mathbb{W}_{i,t}$ and contains the possible values of $w_{t+i} \forall i \in \mathbb{I}_0^\infty$. We, therefore, use $\mathbb{W}_t = \mathbb{W}_0$ to compute a suitable terminal set \mathbb{X}_{TS_t} for formulating the COCP [27], provided the following standard assumption holds.

Assumption 1 *Given constraint sets \mathbb{X}, \mathbb{U} , and \mathbb{W}_0 , for each $\begin{bmatrix} \hat{A} & \hat{B} \end{bmatrix} \in \Psi$, with the corresponding feedback gain $K(\hat{A}, \hat{B})$ obtained from (3), \exists a non-empty terminal set $\mathbb{X}_{TS}(\hat{A}, \hat{B})$ such that*

$$\mathbb{X}_{TS} \subseteq \mathbb{X}, \quad K\mathbb{X}_{TS} \subseteq \mathbb{U}, \quad (10a)$$

$$(\hat{A} + \hat{B}K)\mathbb{X}_{TS} \oplus \mathbb{W}_0 \subseteq \mathbb{X}_{TS}, \quad (10b)$$

and \mathbb{X}_{TS} contains the origin in its interior.

The ideal choice of $\mathbb{X}_{TS_t} = \mathbb{X}_{TS_0}$ is the maximal admissible RPI set satisfying (10); this can be computed following [6] for $\hat{A}_t = \hat{A}_0, \hat{B}_t = \hat{B}_0$ and $K_t = K_0$. Note that the terminal set \mathbb{X}_{TS_t} along with K_t obtained from (3) are specific to a given parameter estimate (\hat{A}_0, \hat{B}_0) , thereby relaxing the requirement for a common pair (P_{com}, K_{com}) and a common terminal set for all the elements in Ψ , unlike [3, 7–9, 13, 19, 21–23, 30]. Even when a common stabilizing feedback gain exists, constructing a common terminal set satisfying (10) for all admissible systems can be difficult or may lead to excessive conservatism. This further motivates the use of terminal ingredients tailored to the current parameter estimate.

3.3 Homothetic tube parameterization

The tubes for state and control input obtained by solving the COCP at each time t are denoted by

$$\mathcal{T}_t^x \triangleq \{\mathbb{T}_{i|t}^x\}_{i=0:N} \quad \text{and} \quad \mathcal{T}_t^u \triangleq \{\mathbb{T}_{i|t}^u\}_{i=0:N-1}, \quad (11)$$

respectively. For the ease of solving the COCP, the tube-sections in \mathcal{T}_t^x are defined as

$$\mathbb{T}_{i|t}^x \triangleq \alpha_{i|t} \oplus \beta_{i|t} \mathbb{S}_t \subseteq \mathbb{X}_{i,t} \quad \forall i \in \mathbb{I}_0^N, \quad (12)$$

where $\alpha_{i|t} \in \mathbb{R}^n$ is the center, $\beta_{i|t} \geq 0$ is the scaling factor, and \mathbb{S}_t determines the tube geometry. The set \mathbb{S}_t is defined to be the convex hull of user-defined vertices $s_t^{[1]}, s_t^{[2]}, \dots, s_t^{[M_t]}$, where M_t is finite. The state tube-sections can also be expressed as

$$\mathbb{T}_{i|t}^x = \mathbf{co} \left(\left\{ z_{i|t}^{[j]} \right\}_{j=1:M_t} \right), \quad \text{where} \quad (13a)$$

$$z_{i|t}^{[j]} \triangleq \alpha_{i|t} + \beta_{i|t} s_t^{[j]} \quad \forall (i, j, t) \in \mathbb{I}_0^N \times \mathbb{I}_1^{M_t} \times \mathbb{I}_0^\infty. \quad (13b)$$

Further, to achieve desirable guarantees of stability and recursive feasibility, a suitable choice of \mathbb{S}_t [7, 27] is that it contains the origin in its interior and is the outer RPI approximation of the minimal RPI set satisfying

$$(\hat{A}_t + \hat{B}_t K_t) \mathbb{S}_t \oplus \mathbb{W}_t \subseteq \mathbb{S}_t. \quad (14)$$

Here, K_t is the feedback gain obtained by solving (3) for \hat{A}_t, \hat{B}_t , and \mathbb{S}_t can be computed following [26]. Again, without any adaptation, we have $\mathbb{S}_t = \mathbb{S}_0 \forall t \in \mathbb{I}_0^\infty$.

Corresponding to (13a), the control tube-sections are written as

$$\mathbb{T}_{i|t}^u \triangleq \left\{ v_{i|t}^{[j]} \right\}_{j=1:M_t} \quad \forall (i, t) \in \mathbb{I}_0^{N-1} \times \mathbb{I}_0^\infty. \quad (15)$$

Since the tube-sections are expressed as convex hulls of vertices, any point $\eta \in \mathbb{T}_{i|t}^x$, can be expressed as $\eta = \sum_{j=1}^{M_t} \tau_{(i,t)}^{[j]} z_{i|t}^{[j]}$, where $\tau_{(i,t)}^{[j]} \in [0, 1]$ and $\sum_{j=1}^{M_t} \tau_{(i,t)}^{[j]} = 1$. The corresponding control input u as a function of η is given by the following function

$$u = \mathbf{u}(\eta, \mathbb{T}_{i|t}^x, \mathbb{T}_{i|t}^u) \triangleq \sum_{j=1}^{M_t} \tau_{(i,t)}^{[j]} v_{i|t}^{[j]}. \quad (16)$$

4 Adaptive tube MPC framework

In this section, we introduce parameter learning and reformulate the COCP with recursive feasibility and stability guarantees. The dynamics used for developing the framework is given by (4)

$$x_{t+1} = \hat{A}_t x_t + \hat{B}_t u_t + w_t,$$

where $w_t \in \mathbb{W}_t$ defined in (6). The suffix t was already introduced with the estimated parameters and sets characterized in the previous section to indicate their time-varying nature due to adaptation. Below, we provide the

laws for carrying out the adaptation of the parameter estimates $\hat{\psi}_t \triangleq \begin{bmatrix} \hat{A}_t & \hat{B}_t \end{bmatrix}$ and the uncertainty set Ψ_t .

4.1 Parameter learning and uncertainty set refinement

At each time step $t \in \mathbb{I}_1^\infty$, the available data x_t, x_{t-1}, u_{t-1} are leveraged to compute a non-falsified set for the true parameter $\psi = \begin{bmatrix} A & B \end{bmatrix}$ as follows [15]

$$\Xi_t \triangleq \left\{ \begin{bmatrix} \hat{A} & \hat{B} \end{bmatrix} \mid x_t - \hat{A}x_{t-1} - \hat{B}u_{t-1} \in \mathbb{D} \right\}. \quad (17)$$

The parametric uncertainty set is then updated as

$$\Psi_t \triangleq \Psi_{t-1} \cap \Xi_t \quad \forall t \in \mathbb{I}_1^\infty; \quad \Psi_0 = \Psi. \quad (18)$$

Lemma 2 *For the plant dynamics (1), the true parameter $\psi = \begin{bmatrix} A & B \end{bmatrix} \in \Psi_t \forall t \in \mathbb{I}_1^\infty$, where the uncertainty sets Ψ_t , obtained using (17) and (18), are nested, i.e., $\Psi_t \subseteq \Psi_{t-1} \forall t \in \mathbb{I}_1^\infty$. This further implies that $\Psi_t \neq \emptyset$ at any time t .*

Proof: The proof easily follows from the plant dynamics (1) and the non-falsified set definition in (17) and the recursive update law (18), since both Ψ_0 and $\Xi_t \forall t \in \mathbb{I}_0^\infty$ contain the true parameter ψ . ■

Since the updated uncertainty set may yield a new set of vertices, we add a time index to the vertices of Ψ_t .

$$\Psi_t = \mathbf{co} \left(\left\{ \psi_t^{[i]} \right\}_{i=1:L_t} \right) \quad \forall t \in \mathbb{I}_0^\infty, \text{ with} \quad (19)$$

$$\psi_0^{[i]} \triangleq \psi^{[i]} \quad \forall i \in \mathbb{I}_1^{L_0}, \text{ where } L_0 \triangleq L.$$

Using the updated uncertainty set Ψ_t , obtained with (18), we compute the point estimate $\hat{\psi}_t$ using a normalized gradient descent-based law along with a projection operator that projects the estimates onto the uncertainty set Ψ_t . To this end, we rewrite (1) as

$$x_t = \psi g_{t-1} + d_{t-1} \quad \forall t \in \mathbb{I}_1^\infty, \quad (20)$$

where $g_{t-1} \triangleq \begin{bmatrix} x_{t-1}^\top & u_{t-1}^\top \end{bmatrix}^\top \in \mathbb{R}^{n+m}$. Here (20) is in a linear regression form with a perturbation-like term d_{t-1} , and at any time t , we know the terms x_t and g_{t-1} . Accordingly the update law is given by

$$\bar{\psi}_t = \hat{\psi}_{t-1} + \kappa \frac{(x_t - \hat{\psi}_{t-1} g_{t-1}) g_{t-1}^\top}{1 + g_{t-1}^\top g_{t-1}}, \quad (21)$$

$$\hat{\psi}_t = \begin{cases} \bar{\psi}_t, & \text{if } \bar{\psi}_t \in \Psi_t \\ \arg \min_{\xi \in \Psi_t} \|\xi - \bar{\psi}_t\|_F, & \text{otherwise,} \end{cases}$$

where $\kappa \in (0, 2)$.

Lemma 3 *Let $e_t \triangleq (x_t - \hat{\psi}_{t-1} g_{t-1}) / (1 + g_{t-1}^\top g_{t-1})$. The update law in (21) with $\kappa \in (0, 2)$ guarantees*

- $e_t, e_t(1 + g_{t-1}^\top g_{t-1})^{\frac{1}{2}}, \hat{\psi}_t \in \mathcal{L}_\infty$,
- $e_t, e_t(1 + g_{t-1}^\top g_{t-1})^{\frac{1}{2}}, \|\hat{\psi}_t - \hat{\psi}_{t-1}\|_F \in \mathcal{S}(\bar{d}^2)$, where \bar{d} is the upper bound of $\|d_t(1 + g_{t-1}^\top g_{t-1})^{-\frac{1}{2}}\|_2$.

Proof: The proof follows from [7, Lemma 1], [12, Theorem 4.11.4] with the use of Lemma 2. ■

4.2 Reformulated COCP with adaptation

Due to the adaptation of Ψ_t and the parameter estimate $\hat{\psi}_t = \begin{bmatrix} \hat{A}_t & \hat{B}_t \end{bmatrix}$, the system dynamics in (4) and the associated sets defined in (5a)-(6) and (7b)-(9) are updated whenever Ψ_t and/or $\hat{\psi}_t$ change. Accordingly, the matrices P_t, K_t , the terminal set \mathbb{X}_{TS_t} and the polytope \mathbb{S}_t defining the tube cross-sectional shape are recomputed to remain consistent with the updated uncertainty description. While this introduces additional computational effort, it enables the controller to exploit any reduction in the size of Ψ_t , leading to the following dual benefits.

- The terminal set, which is desirably the maximal admissible RPI set, increases in size, implying the need for reduced control effort to reach the terminal set, and
- The tube cross-sectional shape \mathbb{S}_t reduces in size, allowing for a better representation of the uncertainty in the propagation of the true state.

The use of updated parameter estimates and uncertainty sets yields a modified COCP at each time instant. However, the switching from the old setup at $t-1$ to the new COCP at t with updated (P_t, K_t) and terminal set \mathbb{X}_{TS_t} may affect recursive feasibility and stability. The treatment of feasibility under such switching is discussed in the next subsection. To ensure stability guarantees, we impose certain conditions on the choice of (P_t, K_t) .

Criterion 4 *Given the parameters \hat{A}_t, \hat{B}_t , the pair (P_{t-1}, K_{t-1}) and matrices Q, R , where $Q, R, P_{t-1} \succ 0$, and constraint sets \mathbb{X}, \mathbb{U} and \mathbb{W}_t , choose a pair (P_t, K_t) that satisfies $P_t \succ 0$ and the following conditions.*

$$(a) \quad P_t - (\hat{A}_t + \hat{B}_t K_t)^\top P_t (\hat{A}_t + \hat{B}_t K_t) - Q - K_t^\top R K_t \succeq 0 \quad (22a)$$

$$(b) \quad P_{t-1} - (\hat{A}_t + \hat{B}_t K_t)^\top P_t (\hat{A}_t + \hat{B}_t K_t) - Q - K_{t-1}^\top R K_{t-1} \succeq 0, \quad (22b)$$

and, (c) \exists a non-empty terminal set \mathbb{X}_{TS_t} such that

$$\mathbb{X}_{TS_t} \subseteq \mathbb{X}, \quad K_t \mathbb{X}_{TS_t} \subseteq \mathbb{U}, \quad (22c)$$

$$(\hat{A}_t + \hat{B}_t K_t) \mathbb{X}_{TS_t} \oplus \mathbb{W}_t \subseteq \mathbb{X}_{TS_t}, \quad (22d)$$

and \mathbb{X}_{TS_t} contains the origin in its interior.

Condition (b) plays a crucial role in preserving stability under adaptation. Specifically, it ensures that the Lyapunov function, which is associated with the cost matrices Q , R , and P_{t-1} at time $t-1$ and P_t at time t , does not increase when the prediction model switches from $(\hat{A}_{t-1}, \hat{B}_{t-1})$ to (\hat{A}_t, \hat{B}_t) and the feedback gain is updated from K_{t-1} to K_t . In other words, even though the terminal cost and prediction dynamics are modified, the value function remains non-increasing along system trajectories, thereby preserving the stability guarantee across switching instances. In the absence of adaptation, i.e., when $(\hat{A}_t, \hat{B}_t) = (\hat{A}_{t-1}, \hat{B}_{t-1})$, Condition (b) reduces to Condition (a), and the requirement coincides with the standard discrete-time Lyapunov inequality for classical MPC [17, Ch. 2].

Conditions (a) and (c) follow from (3) as a property of Ψ_0 and Assumption 1, respectively. Unlike the quadratic stabilizability assumption, which requires the existence of a common pair (P_{com}, K_{com}) satisfying $P_{com} - (\hat{A} + \hat{B}K_{com})^\top P_{com} (\hat{A} + \hat{B}K_{com}) - Q - K_{com}^\top R K_{com} \succeq 0$, $\forall [\hat{A} \ \hat{B}] \in \Psi$, together with a common terminal set, Condition (b) only enforces a one-step compatibility between consecutive parameter updates. Thus, it avoids the need for a common Lyapunov function and feedback gain that are valid for the entire uncertainty set.

Provided Criterion 4 holds, we compute the polytope \mathbb{S}_t as the outer RPI approximation of the minimal RPI set satisfying (14).

Remark 5 *If Criterion 4 does not hold, the point estimates \hat{A}_t, \hat{B}_t and the pair (P_t, K_t) remain unchanged. Nevertheless, adaptation may still occur through contraction of the uncertainty set.*

The COCP for adaptive tube MPC with decision variable $\bar{\mu}_t \triangleq \left\{ \{(\alpha_{i|t}, \beta_{i|t})\}_{i=0:N}, \{v_{i|t}^{[j]}\}_{i=0:N-1, j=1:M_t} \right\}$ is given by

$$\mathbb{P}2_t : \min_{\bar{\mu}_t} \sum_{j=1}^{M_t} \left(\sum_{i=0}^{N-1} \left(\|z_{i|t}^{[j]}\|_Q^2 + \|v_{i|t}^{[j]}\|_R^2 \right) + \|z_{N|t}^{[j]}\|_{P_t}^2 \right) \quad (24a)$$

subject to (11) – (13)

$$\beta_{i|t} \geq 0 \quad \forall i \in \mathbb{I}_1^N, \quad (24b)$$

$$\mathbb{T}_{0|t}^x = \{x_t\}, \quad (24c)$$

$$\mathbb{T}_{i|t}^x \subseteq \mathbb{X}, \mathbb{T}_{i|t}^u \subseteq \mathbb{U} \quad \forall i \in \mathbb{I}_0^{N-1}, \quad (24d)$$

$$\mathbb{T}_{N|t}^x \subseteq \mathbb{X}_{TS_t} \subseteq \mathbb{X}, \text{ and} \quad (24e)$$

$$\hat{A}_t z_{i|t}^{[j]} + \hat{B}_t v_{i|t}^{[j]} \in \mathbb{T}_{i+1|t}^x \ominus \mathbb{W}_{i,t} \quad \forall (i, j) \in \mathbb{I}_0^{N-1} \times \mathbb{I}_1^{M_t}. \quad (24f)$$

Using the solution of the COCP and (16), we compute the input $u_t^* = \mathbf{u}(x_t, \mathbb{T}_{i|t}^{x^*}, \mathbb{T}_{i|t}^{u^*})$ that is applied to the plant (1) to evolve to the next state x_{t+1} . The COCP is labelled as $\mathbb{P}2_t$ since the formulation depends on time t .

It is possible that the new set Ψ_t , with the new estimates \hat{A}_t, \hat{B}_t and the consequently computed sets, leads to an infeasible COCP. First, there may not exist a (P_t, K_t) that satisfies Criterion 4. Second, even if Criterion 4 holds, (24) may be infeasible due to the inadequate length of the prediction horizon. In either case, we revert to the previous estimates by setting $\hat{A}_t \leftarrow \hat{A}_{t-1}, \hat{B}_t \leftarrow \hat{B}_{t-1}, P_t \leftarrow P_{t-1}, K_t \leftarrow K_{t-1}$ and

$$\Psi_t \leftarrow \text{co} \left(\Psi_t, \left\{ [\hat{A}_{t-1} \ \hat{B}_{t-1}] \right\} \right), \quad (25)$$

and compute the sets in (5a)-(6), (7b)-(9), \mathbb{X}_{TS_t} and \mathbb{S}_t . At any time step, if there is a change in the set Ψ_t or the estimates \hat{A}_t, \hat{B}_t , the shape of the disturbance-related sets along with the polytope \mathbb{S}_t changes. This renders the tube an *adaptive* nature, allowing for improved characterization of the uncertainties in trajectory propagation of the true system (1). Algorithm 1 outlines the steps for implementing the proposed framework.

Remark 6 *It is possible that the number of vertices of Ψ_t may increase with t . To ensure that the approach is tractable, one can either stop the set adaptation after the number of vertices L_t reaches a pre-decided upper bound depending on the computational resources or opt for methods discussed in [4, 21, 28].*

Remark 7 *According to Algorithm 1, if $\mathbb{P}2_t$ is infeasible at some time $t \in \mathbb{I}_1^\infty$, the COCP is reformulated using the setup described in Steps 28-30 and solved with the updated formulation. To avoid the additional computational effort associated with resolving the modified problem at time t , the control input u_t can instead be computed using the previously obtained optimal solution at time $t-1$, together with the measured state x_t and (16).*

4.3 Recursive Feasibility and Stability Analysis

Next, we prove that the proposed COCP $\mathbb{P}2_t$ following Algorithm 1 is recursively feasible, and leads to robust exponential stability of the origin of (1).

Theorem 8 *Suppose Assumption 1 holds, and the COCP $\mathbb{P}2_t$ is feasible at some time t . Then, Algorithm 1 ensures that $\mathbb{P}2_t$ is feasible at time $t+k \forall k \in \mathbb{I}_1^\infty$.*

Proof: The proof proceeds by induction. Assume that the COCP is feasible at time t . We show feasibility at time $t+1$.

Given a feasible solution at t , the plant (1) evolves and the parameter estimates, uncertainty set and distur-

Algorithm 1 Adaptive Tube MPC

Input: $\mathbb{X}, \mathbb{U}, \mathbb{D}, \psi^{[i]} \forall i \in \mathbb{I}_1^{L_0}, N, Q, R, \hat{\psi}_0, \kappa$.

Output: $\hat{\mu}_t^* \forall t \in \mathbb{I}_0^\infty$.

Steps:

- 1: Initialize $\Psi_0 = \Psi$, i.e., $\psi_0^{[i]} = \psi^{[i]} \forall i \in \mathbb{I}_1^{L_0}$, a constant $c_{\text{backup}} = 0$ and time $t = 0$.
 - 2: Measure x_0 .
 - 3: **while** $t \geq 0$ **do**
 - 4: Compute $\Phi_t, \Phi_{A_t}, \Phi_{B_t}, \mathbb{W}_t, \Psi_{A_t}, \Psi_{B_t}$, and $\mathbb{X}_{i,t}, \mathbb{W}_{i,t} \forall i \in \mathbb{I}_0^{N-1}$ and \mathbb{S}_t using (5a)-(9) and (14).
 - 5: **if** $t == 0$ **then**
 - 6: Choose P_t, K_t and \mathbb{X}_{TS_t} that satisfies (3) and Assumption 1.
 - 7: **else**
 - 8: Check if $\exists P_t, K_t, \mathbb{X}_{TS_t}$ satisfying Criterion 4.
 - 9: **if** Criterion 4 does not hold **then**
 - 10: Set $c_{\text{backup}} \leftarrow 1, t \leftarrow t - 1$ and go to Step 28.
 - 11: **end if**
 - 12: **end if**
 - 13: Run the COCP $\mathbb{P}2_t$.
 - 14: **if** $\hat{\mu}_t^* \neq \emptyset$, i.e., $\mathbb{P}2_t$ is feasible **then**
 - 15: Set $c_{\text{backup}} \leftarrow 0$.
 - 16: **else**
 - 17: **if** $t == 0$ **then**
 - 18: Exit the algorithm (initially infeasible).
 - 19: **else**
 - 20: Set $c_{\text{backup}} \leftarrow 1$ and $t \leftarrow t - 1$.
 - 21: **end if**
 - 22: **end if**
 - 23: **if** $c_{\text{backup}} == 0$ **then**
 - 24: Apply $u_t^* = \mathbf{u}(x_t, \mathbb{T}_{i|t}^{x*}, \mathbb{T}_{i|t}^{u*})$ to the plant (1).
 - 25: Measure x_{t+1} from (1).
 - 26: Compute the non-falsified set Ξ_{t+1} , the uncertainty set Ψ_{t+1} , and the point estimate $\hat{\psi}_{t+1}$ using (17), (18), and (21), respectively.
 - 27: **end if**
 - 28: **if** $c_{\text{backup}} == 1$ **then**
 - 29: Compute Ψ_{t+1} using (25), and set $\hat{A}_{t+1} \leftarrow \hat{A}_t, \hat{B}_{t+1} \leftarrow \hat{B}_t, \hat{P}_{t+1} \leftarrow \hat{P}_t, \hat{K}_{t+1} \leftarrow \hat{K}_t$.
 - 30: **end if**
 - 31: Update $t \leftarrow t + 1$.
 - 32: **end while**
-

bance sets are updated. Criterion 4 is then checked at $t + 1$. If it is satisfied, new matrices P_t, K_t , terminal set and tube geometry \mathbb{S}_t are computed, resulting in a modified COCP. Since the problem data change, feasibility of this newly formed problem cannot be guaranteed a priori. If $\mathbb{P}2_{t+1}$ is feasible, the algorithm proceeds with its solution. Otherwise, or if Criterion 4 does not hold, the backup setup in Step 29 is used. For the backup, two situations arise.

- (i) *No update of point estimate or uncertainty set.* In this case, the COCP coincides with the standard homothetic tube-based MPC formulation. Recursive feasibility follows from the existing literature (see [7, 20,

21, 27]). Let the feasible solution at $t + 1$ for the non-adaptive scenario be denoted as follows using $\underline{(\cdot)}$, with $(\cdot)^*$ denoting the optimal solution of \mathbb{P}_t .

$$\underline{\mathbb{T}}_{0|t+1}^x = \{x_{t+1}\}, \quad (26a)$$

$$\underline{\mathbb{T}}_{i|t+1}^x = \mathbb{T}_{i+1|t}^{x*} \quad \forall i \in \mathbb{I}_1^{N-1}, \quad (26b)$$

$$\underline{\mathbb{T}}_{i|t+1}^u = \mathbb{T}_{i+1|t}^{u*} \quad \forall i \in \mathbb{I}_0^{N-2}, \quad (26c)$$

$$\underline{\mathbb{T}}_{N|t+1}^x = \underline{\alpha}_{N|t+1} \oplus \underline{\beta}_{N|t+1} \mathbb{S}_t, \quad (26d)$$

$$\underline{\mathbb{T}}_{N-1|t+1}^x = K_t \underline{\mathbb{T}}_{N-1|t+1}^x = K_t \mathbb{T}_{N|t}^{x*}, \quad (26e)$$

$$\text{where } \underline{\alpha}_{N|t+1} = (\hat{A}_t + \hat{B}_t K_t) \alpha_{N|t}^* \text{ and} \quad (26f)$$

$$\underline{\beta}_{N|t+1} = \min_{\beta} \left\{ \beta \mid (\hat{A}_t + \hat{B}_t K_t) \beta_{N|t}^* \mathbb{S}_t \oplus \mathbb{W}_t \subseteq \beta \mathbb{S}_t \right\}, \quad (26g)$$

with $z_{i|t+1}^{[j]}$ and $v_{i|t+1}^{[j]}$ being the vertices of $\underline{\mathbb{T}}_{i|t+1}^x \forall i \in \mathbb{I}_0^N$ and the elements of $\underline{\mathbb{T}}_{i|t+1}^u \forall i \in \mathbb{I}_0^{N-1}$, respectively, $\forall j \in \mathbb{I}_1^{M_t}$. The solution is useful in proving recursive feasibility of the next case.

- (ii) *Uncertainty set update only.* Here, the point estimates \hat{A}_t, \hat{B}_t and (P_t, K_t) remain unchanged, while the uncertainty set is refined according to (25), yielding $\Psi_{t+1} \subseteq \underline{\Psi}_{t+1} = \Psi_t$. Consequently, $\Phi_{t+1} \subseteq \underline{\Phi}_{t+1} = \Phi_t, \Phi_{A_{t+1}} \subseteq \underline{\Phi}_{A_{t+1}} = \Phi_{A_t}, \Phi_{B_{t+1}} \subseteq \underline{\Phi}_{B_{t+1}} = \Phi_{B_t}, \Psi_{A_{t+1}} \subseteq \underline{\Psi}_{A_{t+1}} = \Psi_{A_t}, \Psi_{B_{t+1}} \subseteq \underline{\Psi}_{B_{t+1}} = \Psi_{B_t}$, resulting in

$$\mathbb{W}_{t+1} \subseteq \underline{\mathbb{W}}_{t+1} = \mathbb{W}_t, \mathbb{S}_{t+1} \subseteq \underline{\mathbb{S}}_{t+1} = \mathbb{S}_t, \quad (27a)$$

$$\mathbb{X}_{i,t+1} \subseteq \underline{\mathbb{X}}_{i,t+1} \subseteq \mathbb{X}_{i+1,t} \quad \forall i \in \mathbb{I}_0^{N-1}, \quad (27b)$$

$$\mathbb{W}_{i,t+1} \subseteq \underline{\mathbb{W}}_{i,t+1} \subseteq \mathbb{W}_{i+1,t} \quad \forall i \in \mathbb{I}_0^{N-1}, \quad (27c)$$

$$\mathbb{X} \supseteq \underline{\mathbb{X}}_{TS_{t+1}} \supseteq \underline{\mathbb{X}}_{TS_{t+1}} = \mathbb{X}_{TS_t}. \quad (27d)$$

Leveraging (27) and the solution (26) for the non-adaptive case, we prove that the following is a feasible solution for the COCP at $t + 1$ under the refined sets.

$$\mathbb{T}_{i|t+1}^x = \alpha_{i|t+1} \oplus \beta_{i|t+1} \mathbb{S}_{t+1} \quad \forall i \in \mathbb{I}_0^N, \text{ where} \quad (28a)$$

$$\alpha_{0|t+1} = x_{t+1}, \beta_{0|t+1} = 0, \quad (28b)$$

$$\alpha_{i|t+1} = \alpha_{i+1|t}^*, \beta_{i|t+1} = \beta_{i+1|t}^* \quad \forall i \in \mathbb{I}_1^{N-1}, \quad (28c)$$

$$\alpha_{N|t+1} = \underline{\alpha}_{N|t+1}, \beta_{N|t+1} = \underline{\beta}_{N|t+1}, \text{ and} \quad (28d)$$

$$\mathbb{T}_{i|t+1}^u = \left\{ \mathbf{u}(z_{i|t+1}^{[j]}, \underline{\mathbb{T}}_{i|t+1}^x, \underline{\mathbb{T}}_{i|t+1}^u) \mid j \in \mathbb{I}_1^{M_{t+1}} \right\}. \quad (28e)$$

It is easily seen that the centers and scaling factors in (28) satisfy (11)-(13), (24b) and (24c) at $t + 1$. For the tube-sections, we can write

$$\mathbb{T}_{0|t+1}^x = \underline{\mathbb{T}}_{0|t+1}^x \subseteq \mathbb{X}_{1,t},$$

$$\begin{aligned}\mathbb{T}_{i|t+1}^x &= \alpha_{i|t+1} \oplus \beta_{i|t+1} \mathbb{S}_{t+1} \\ &\subseteq \alpha_{i+1|t}^* \oplus \beta_{i+1|t}^* \mathbb{S}_t \\ &= \underline{\mathbb{T}_{i|t+1}^x} \subseteq \mathbb{X}_{i+1,t} \quad \forall i \in \mathbb{I}_1^{N-1},\end{aligned}$$

$$\begin{aligned}\mathbb{T}_{N|t+1}^x &= \alpha_{N|t+1} \oplus \beta_{N|t+1} \mathbb{S}_{t+1} \\ &\subseteq \underline{\alpha_{N|t+1}} \oplus \underline{\beta_{N|t+1}} \mathbb{S}_t \\ &= \underline{\mathbb{T}_{N|t+1}^x} \subseteq \mathbb{X}_{TS_t} \subseteq \mathbb{X}_{TS_{t+1}} \subseteq \mathbb{X},\end{aligned}$$

$$\mathbf{co}(\mathbb{T}_{i|t+1}^u) \subseteq \mathbf{co}(\underline{\mathbb{T}_{i|t+1}^u}) \Rightarrow \mathbb{T}_{i|t+1}^u \subseteq \mathbb{U} \quad \forall i \in \mathbb{I}_0^{N-1},$$

which together prove the satisfaction of (24d) and (24e) at time $t + 1$. Finally, for (28) to satisfy (24f), note that from the non-adaptive case we have

$$\hat{A}_t z_{i|t+1}^{[j]} + \hat{B}_t v_{i|t+1}^{[j]} \in \underline{\mathbb{T}_{i+1|t+1}^x} \ominus \underline{\mathbb{W}_{i,t+1}},$$

$\mathbb{S}_{t+1} \subseteq \underline{\mathbb{S}_{t+1}}$, $\mathbb{T}_{i|t+1}^x \subseteq \underline{\mathbb{T}_{i|t+1}^x}$, $\mathbf{co}(\mathbb{T}_{i|t+1}^u) \subseteq \mathbf{co}(\underline{\mathbb{T}_{i|t+1}^u})$, and $\mathbb{W}_{i,t+1} \subseteq \underline{\mathbb{W}_{i,t+1}}$. Since the prediction dynamics is linear and the input applied to any $z \in \mathbb{T}_{i|t+1}^x$ is obtained through the convex-combination mapping (16), it follows that

$$\hat{A}_{t+1} z_{i|t+1}^{[j]} + \hat{B}_{t+1} v_{i|t+1}^{[j]} \in \underline{\mathbb{T}_{i+1|t+1}^x} \ominus \underline{\mathbb{W}_{i,t+1}}.$$

Hence (24f) holds at time $t + 1$, and the proposed solution in (28) satisfies all the constraints in $\mathbb{P}_{2,t+1}$.

Therefore, whenever the backup setup is invoked, a feasible solution to the COCP at time $t + 1$ exists. If Criterion 4 is satisfied, the algorithm instead attempts to solve the updated problem $\mathbb{P}_{2,t+1}$ corresponding to the modified problem data. If this problem is feasible, the resulting solution is applied; otherwise, the backup setup ensures feasibility. Repeating the same argument at subsequent time steps establishes recursive feasibility of the proposed MPC COCP. \blacksquare

Corollary 9 *Suppose Assumption 1 holds, and the COCP $\mathbb{P}_{2,t}$ is feasible at time t . Then, by Lemmas 2, 3 and Theorem 8, it is guaranteed that the signals $x_t, u_t, \hat{\psi}_t \in \mathcal{L}_\infty$.*

Theorem 10 *Suppose Assumption 1 holds, and the COCP $\mathbb{P}_{2,t}$ is feasible at time t . Then, Algorithm 1 guarantees robust exponential stability of the origin of the plant (1).*

Proof: The proof follows the standard MPC stability argument [17] by using the cost function of the COCP as a candidate Lyapunov function. Let the COCP cost

function be denoted as

$$\begin{aligned}J_t(x_t, \bar{\mu}_t) &\triangleq \sum_{j=1}^{M_t} \Gamma_t^{[j]}, \text{ where} \\ \Gamma_t^{[j]} &\triangleq \sum_{i=0}^{N-1} \left(\|z_{i|t}^{[j]}\|_Q^2 + \|v_{i|t}^{[j]}\|_R^2 \right) + \|z_{N|t}^{[j]}\|_{P_t}^2\end{aligned}$$

is the component of the cost function for each vertex of the tube-sections. To address the change in the number of vertices (M_t to M_{t+1}) due to a change in the tube geometry, define the variables

$$\rho_{1t} \triangleq \begin{cases} 0, & \text{if } M_t \leq M_{t+1} \\ 1, & \text{otherwise,} \end{cases} \quad \rho_{2t} \triangleq \begin{cases} 0, & \text{if } M_t \geq M_{t+1} \\ 1, & \text{otherwise.} \end{cases}$$

Also, let

$$\gamma_1 \triangleq \max_{t \in \mathbb{I}_0^\infty, x \in \mathbb{X}, u \in \mathbb{U}} N(\|x\|_Q^2 + \|u\|_R^2) + \|x\|_{P_{t+1}}^2, \quad (29)$$

which by Lemmas 2, 3 and Theorem 8 is finite.

At any time $t + 1$, where $t \in \mathbb{I}_0^\infty$, we can write

$$\begin{aligned}J_{t+1}^*(x_{t+1}) &\leq J_{t+1}(x_{t+1}, \bar{\mu}_{t+1}) = \sum_{j=1}^{M_{t+1}} \Gamma_{t+1}^{[j]} \\ &= \sum_{j=1}^{M_t} \Gamma_{t+1}^{[j]} - \rho_{1t} \sum_{j=M_{t+1}+1}^{M_t} \Gamma_{t+1}^{[j]} + \rho_{2t} \sum_{j=M_{t+1}}^{M_{t+1}} \Gamma_{t+1}^{[j]} \\ &\leq \sum_{j=1}^{M_t} \left(\sum_{i=0}^{N-1} \left(\|z_{i|t+1}^{[j]}\|_Q^2 + \|v_{i|t+1}^{[j]}\|_R^2 \right) + \|z_{N|t+1}^{[j]}\|_{P_{t+1}}^2 \right) \\ &\quad + \rho_{2t} (M_{t+1} - M_t) \gamma_1 \quad (\text{using (29)}) \\ &\leq \sum_{j=1}^{M_t} \left(\sum_{i=0}^{N-1} \left(\|z_{i|t+1}^{[j]}\|_Q^2 + \|v_{i|t+1}^{[j]}\|_R^2 \right) + \|z_{N|t+1}^{[j]}\|_{P_{t+1}}^2 \right) \\ &\quad + \rho_{2t} (M_{t+1} - M_t) \gamma_1 \\ &\quad \left(\because \mathbb{T}_{i|t+1}^x \subseteq \underline{\mathbb{T}_{i|t+1}^x}, \mathbf{co}(\mathbb{T}_{i|t+1}^u) \subseteq \mathbf{co}(\underline{\mathbb{T}_{i|t+1}^u}) \right) \\ &= \sum_{j=1}^{M_t} \left(\sum_{i=0}^{N-2} \left(\|z_{i+1|t}^{[j]*}\|_Q^2 + \|v_{i+1|t}^{[j]*}\|_R^2 \right) + \|z_{N|t+1}^{[j]}\|_{P_{t+1}}^2 \right) \\ &\quad + \|z_{N|t}^{[j]*}\|_{Q+K_t^\top R K_t}^2 + \rho_{2t} (M_{t+1} - M_t) \gamma_1 \quad (\text{using (26)}) \\ &= J_t^*(x_t) - \sum_{j=1}^{M_t} \left(\|z_{0|t}^{[j]*}\|_Q^2 + \|v_{0|t}^{[j]*}\|_R^2 + \|z_{N|t}^{[j]*}\|_{P_t}^2 \right) \\ &\quad + \sum_{j=1}^{M_t} \left(\|(\hat{A}_{t+1} + \hat{B}_{t+1} K_{t+1}) z_{N|t}^{[j]*} + w_{t+N}\|_{P_{t+1}}^2 \right. \\ &\quad \left. + \|z_{N|t}^{[j]*}\|_{Q+K_t^\top R K_t}^2 \right) + \rho_{2t} (M_{t+1} - M_t) \gamma_1\end{aligned}$$

$$\begin{aligned}
&\leq (1 - \gamma_2)J_t^*(x_t) + \sum_{j=1}^{M_t} \left(-\|z_{N|t}^{[j]*}\|_{P_t}^2 + \|z_{N|t}^{[j]*}\|_{Q+K_t^\top RK_t}^2 \right. \\
&\quad \left. + \|z_{N|t}^{[j]*}\|_{(\hat{A}_{t+1} + \hat{B}_{t+1}K_{t+1})^\top P_{t+1}(\hat{A}_{t+1} + \hat{B}_{t+1}K_{t+1})}^2 \right) \\
&\quad + M_t \max_{t \in \mathbb{I}_0^\infty, w \in \mathbb{W}_t} \|w\|_{P_{t+1}}^2 + \rho_{2_t}(M_{t+1} - M_t)\gamma_1, \\
&\quad \text{(by Cauchy-Schwartz inequality)}
\end{aligned}$$

where $\sum_{j=1}^{M_t} \left(\|z_{0|t}^{[j]*}\|_Q^2 + \|v_{0|t}^{[j]*}\|_R^2 \right) = \gamma_2 J_t^*(x_t)$, implying $\gamma_2 \in (0, 1] \Rightarrow 1 - \gamma_2 \in [0, 1)$ (by definition of J_t^*).

Since the COCP is initially feasible and Assumption 1 holds, by Theorem 8, recursive feasibility is guaranteed. Either Criterion 4 is satisfied, or we revert to $\hat{A}_{t+1} = \hat{A}_t$, $\hat{B}_{t+1} = \hat{B}_t$, $P_{t+1} = P_t$ and $K_{t+1} = K_t$ that satisfies (3). In any case, we have

$$\begin{aligned}
&P_t - (\hat{A}_{t+1} + \hat{B}_{t+1}K_{t+1})^\top P_{t+1}(\hat{A}_{t+1} + \hat{B}_{t+1}K_{t+1}) \\
&\quad - Q - K_t^\top RK_t \succeq 0, \\
\Rightarrow J_{t+1}^*(x_{t+1}) &\leq (1 - \gamma_2)J_t^*(x_t) + \rho_{2_t}(M_{t+1} - M_t)\gamma_1 \\
&\quad + M_t \max_{t \in \mathbb{I}_0^\infty, w \in \mathbb{W}_t} \|w\|_{P_{t+1}}^2.
\end{aligned}$$

For implementation purposes, we put an upper limit M_{max} on the number of vertices \mathbb{S}_t , depending on the computational power. Due to recursive feasibility and bounded sets \mathbb{D} and Ψ_t , the value of w_t is upper bounded. The elements of P_t are also upper bounded, since P_t is involved in the cost function. Therefore, we can define a constant $\gamma_3 \triangleq M_{max} \max_{t \in \mathbb{I}_0^\infty, w \in \mathbb{W}_t} \|w\|_{P_t}^2 + (M_{max} - M_{min})\gamma_1$ resulting in

$$J_{t+1}^*(x_{t+1}) \leq (1 - \gamma_2)J_t^*(x_t) + \gamma_3, \quad (30)$$

which implies the plant (1) exhibits robust exponential stability. Further, once the learning has converged, M_t remains constant and the term $M_{t+1} - M_t$ becomes 0, implying that the state eventually converges to a finite set that depends on the sizes of \mathbb{D} and Ψ_t and \hat{A}_t, \hat{B}_t as $t \rightarrow \infty$, all of which are bounded (see Corollary 9). ■

5 Numerical Example

We validate the proposed MPC framework using the following 2nd order LTI system².

$$x_{t+1} = \begin{bmatrix} 0.2 & 1.015 \\ -0.2825 & 1 \end{bmatrix} x_t + \begin{bmatrix} 1.08 \\ 3 \end{bmatrix} u_t + d_t$$

with $\|d_t\|_\infty \leq 0.1$ and constraints $\|x_t\|_\infty \leq 20$, $\|u_t\|_\infty \leq 10$. The parametric uncertainty is considered

² A 2nd order system is chosen for ease of visualizing the tubes.

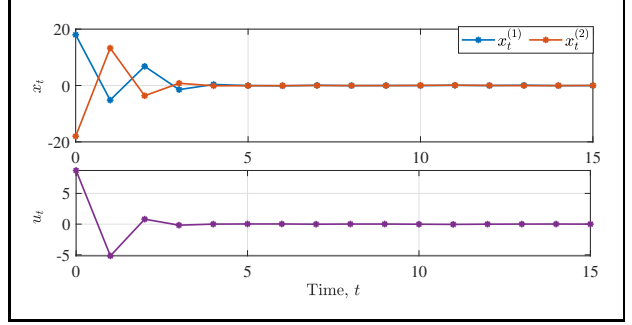


Fig. 1. State and control input.

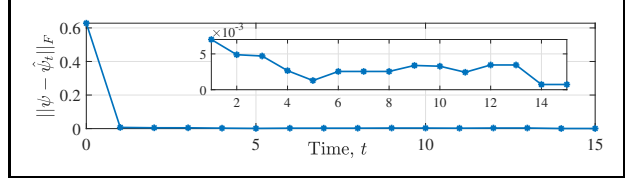


Fig. 2. Frobenius norm of the parameter estimation error.

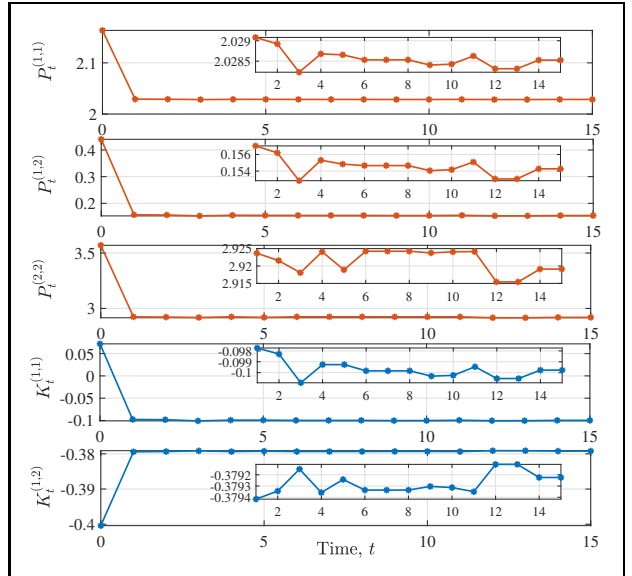


Fig. 3. Elements of the terminal cost weight matrix, and the stabilizing linear feedback gain.

in two elements of A and one element of B with 3 vertices of Ψ given by $\psi^{[1]} = [0.2 \ 1.3 \ 0.7; -1 \ 1 \ 3]$, $\psi^{[2]} = [0.2 \ 1.2 \ 0.9; -0.25 \ 1 \ 3]$, $\psi^{[3]} = [0.2 \ 1 \ 1.1; 0.35 \ 1 \ 3]$. The results in Figs 1-8 are provided for $x_0 = [18; -18]$, $N = 10$, $Q = [1 \ 0; 0 \ 1]$, $R = 0.1$ and $\kappa = 0.9$ with $\hat{\psi}_0 = (\psi^{[1]} + \psi^{[2]} + \psi^{[3]})/3$.

It is seen from Fig. 1 that the hard constraints in (2) are satisfied, and the state trajectory converges to the neighbourhood of the origin. The parameter estimation error norm is bounded as shown in Fig. 2, and the variations in the elements of P_t and K_t are shown in Fig. 3.

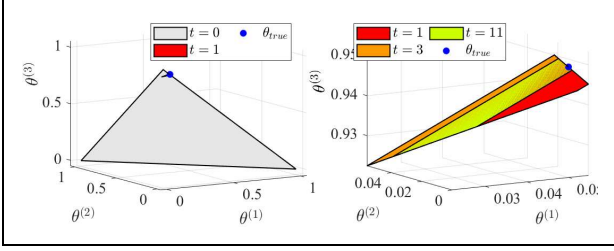


Fig. 4. Barycentric representation of the parametric uncertainty sets containing the convex combination of the true parameter (shown with a blue dot).

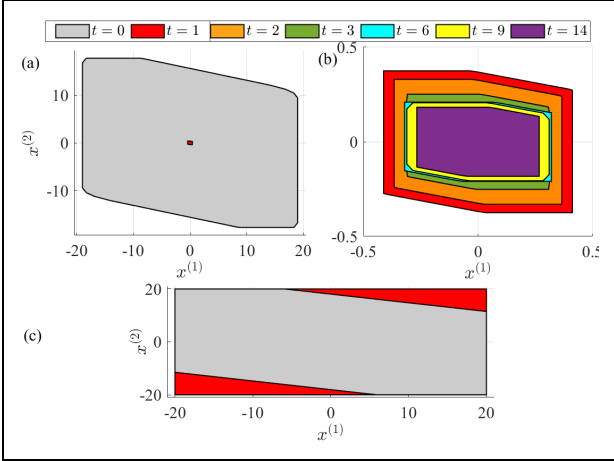


Fig. 5. (a), (b) The polytopes used to define the cross-sectional shape of the homothetic tubes, (c) The terminal sets.

The reduction of the size of the parametric uncertainty set Ψ_t at $t = 1, 3, 11$ is shown in Fig. 4. From Fig. 5 (a), (b) and (c), the adaptation in the shape of the homothetic tube \mathbb{S}_t and the terminal set \mathbb{X}_{TS_t} is visible. The shape of \mathbb{S}_t changes and the size reduces, giving a better characterization of state propagation in the presence of uncertainty Ψ_t and \mathbb{D} , whereas the terminal set size increases thereby reducing the strain on the controller to reach the terminal set. To highlight the impact of tube adaptation, the performance of the proposed MPC is compared with the robust homothetic tube MPC scheme of [27]. The comparison focuses on the amount of constraint tightening required to guarantee robustness, the stabilization performance and the associated stage cost.

Fig. 6 shows the predicted state tubes at selected time instants. The first and second subplots correspond to the tubes generated at $t = 0$ and $t = 1$, respectively. The tube produced by the proposed adaptive method (shown in green) is noticeably smaller than the tubes obtained using the robust homothetic tube MPC method of [27] (shown with magenta outline). This reduction in tube size is a direct consequence of the contraction of the parametric uncertainty set through online learning.

The second subplot further shows that the tube generated by the proposed method without adaptation (blue

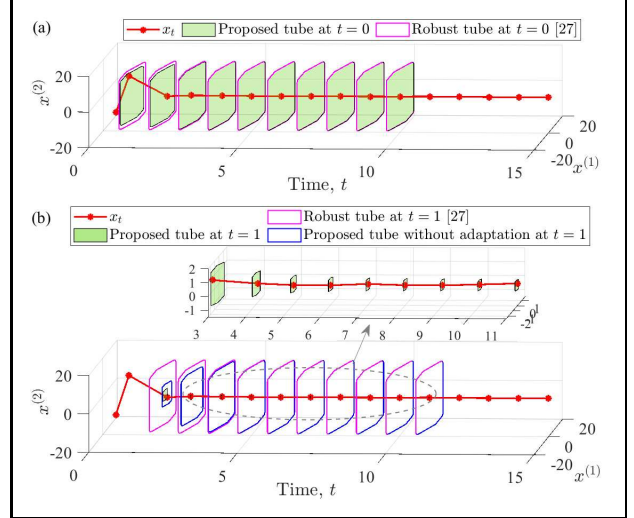


Fig. 6. Tubes generated at $t = 0$ and $t = 1$ following the proposed framework and [27], along with the state trajectory generated with the proposed method.

outline) is still smaller than the tube generated following [27]. This is because even without adaptation, the disturbance set characterization is improved at each time step, whereas the robust tube MPC scheme relies on a fixed set that accounts for all admissible disturbance w_t , thereby leading to larger tube cross-sections.

The tightening sets associated with the disturbance bounds are illustrated in Figs 7 (a) and (b) for $t = 0$ and $t = 1$, respectively. The tightening set used by the method of [27] is shown in grey in Fig. 7 (a) and remains fixed over time. In contrast, the tightening sets generated by the proposed method, shown in Fig. 7 (a) and (b), shrink as the parametric uncertainty set is refined through learning. This reduction enlarges the region available for the state trajectory to evolve while maintaining robust constraint satisfaction.

The improvement in performance is reflected in Fig. 8. The figure shows the evolution of the state norm $\|x_t\|_2$ and the cumulative stage cost for the proposed method and the robust tube MPC scheme of [27]. The proposed adaptive scheme achieves a faster reduction of the state norm, indicating improved stabilization performance. In addition, the cumulative stage cost is lower, reflecting a reduction in control effort enabled by the improved model representation obtained through online learning.

These results demonstrate that adapting the tube geometry and other COCP components through online refinement of the uncertainty set significantly reduces conservatism while maintaining robust constraint satisfaction.

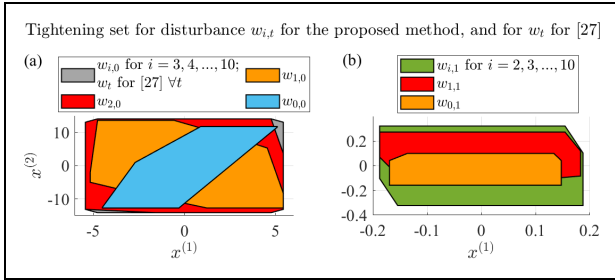


Fig. 7. Sets used for constraint tightening corresponding to the disturbance bounds for the proposed adaptive method and the robust tube MPC [27].

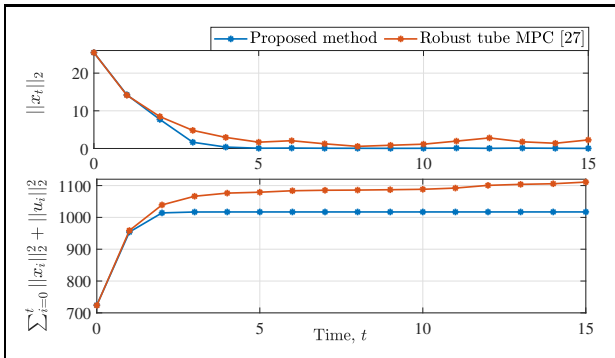


Fig. 8. Comparison of $\|x_t\|_2$ and the cumulative stage cost for the proposed method and [27].

6 Conclusion

This paper introduces an adaptive tube framework for MPC of discrete-time LTI systems subject to parametric uncertainty and additive disturbances. The approach integrates homothetic tube-based MPC with set-membership identification, allowing the parametric uncertainty set and parameter estimates to be updated online using available state and input data. As the uncertainty set contracts, the tube cross-sections adapt accordingly, leading to less conservative constraint tightening and state propagation. It is formally established that the resulting adaptive tube MPC scheme guarantees recursive feasibility, robust exponential stability, and boundedness of all signals, despite the time-varying nature of the COCP induced by adaptation. A key theoretical feature of the framework is that it avoids the standard assumption of a common quadratically stabilizing linear feedback gain for the entire parametric uncertainty set, instead requiring only a one-step Lyapunov compatibility condition between consecutive parameter updates. A backup mechanism ensures that these guarantees are preserved even when the adaptive updates render the modified COCP infeasible. Numerical results demonstrate the benefits of the adaptive tube construction in reducing conservatism and improving performance. Future work will focus on reducing the computational burden associated with online recomputation of tube and terminal ingredients and extending

the framework to the output feedback scenario.

References

- [1] B Ross Barmish. Necessary and sufficient conditions for quadratic stabilizability of an uncertain system. *Journal of Optimization theory and applications*, 46(4):399–408, 1985.
- [2] Julian Berberich, Johannes Köhler, Matthias A Müller, and Frank Allgöwer. Data-driven model predictive control with stability and robustness guarantees. *IEEE Transactions on Automatic Control*, 66(4):1702–1717, 2020.
- [3] Monimoy Bujarbaruah, Ugo Rosolia, Yvonne R. Stürz, and Francesco Borrelli. A simple robust MPC for linear systems with parametric and additive uncertainty. In *American Control Conference*, pages 2108–2113, 2021.
- [4] L. Chisci, J.A. Rossiter, and G. Zappa. Systems with persistent disturbances: predictive control with restricted constraints. *Automatica*, 37(7):1019–1028, 2001.
- [5] Jeremy Coulson, John Lygeros, and Florian Dörfler. Data-enabled predictive control: In the shallows of the DeePC. In *European Control Conference*, pages 307–312, 2019.
- [6] Anchita Dey and Shubhendu Bhasin. Computation of maximal admissible robust positive invariant sets for linear systems with parametric and additive uncertainties. *IEEE Control Systems Letters*, 8:1775–1780, 2024.
- [7] Anchita Dey and Shubhendu Bhasin. Adaptive output feedback MPC with guaranteed stability and robustness. *IEEE Transactions on Automatic Control*, 70(12):8345–8352, 2025.
- [8] Anchita Dey, Abhishek Dhar, and Shubhendu Bhasin. Adaptive output feedback model predictive control. *IEEE Control Systems Letters*, 7:1129–1134, 2023.
- [9] Abhishek Dhar and Shubhendu Bhasin. Indirect adaptive MPC for discrete-time LTI systems with parametric uncertainties. *IEEE Transactions on Automatic Control*, 66(11):5498–5505, 2021.
- [10] James Fleming, Basil Kouvaritakis, and Mark Cannon. Robust tube MPC for linear systems with multiplicative uncertainty. *IEEE Transactions on Automatic Control*, 60(4):1087–1092, 2015.
- [11] Pascal Gahinet and Pierre Apkarian. A linear matrix inequality approach to H_∞ control. *International Journal of Robust and Nonlinear Control*, 4(4):421–448, 1994.
- [12] Petros Ioannou and Barış Fidan. *Adaptive Control Tutorial*. SIAM, 2006.
- [13] Sh Jafari Fesharaki, M Kamali, and F Sheikholeslam. Adaptive tube-based model predictive control for linear systems with parametric uncertainty. *IET Control Theory & Applications*, 11(17):2947–2953, 2017.
- [14] Pramod P Khargonekar, Ian R Petersen, and Kemin Zhou. Robust stabilization of uncertain linear systems: quadratic stabilizability and H_∞ control theory. *IEEE Transactions on Automatic Control*, 35(3):356–361, 1990.
- [15] R.L. Kosut, M.K. Lau, and S.P. Boyd. Set-membership identification of systems with parametric and nonparametric uncertainty. *IEEE Transactions on Automatic Control*, 37(7):929–941, 1992.
- [16] Mayuresh V. Kothare, Venkataramanan Balakrishnan, and Manfred Morari. Robust constrained model predictive control using linear matrix inequalities. *Automatica*, 32(10):1361–1379, 1996.

- [17] Basil Kouvaritakis and Mark Cannon. Model Predictive Control. *Cham, Switzerland: Springer International*, 38, 2016.
- [18] Markus Kögel and Rolf Findeisen. Robust MPC with reduced conservatism blending multiples tubes. In *American Control Conference*, pages 1949–1954, 2020.
- [19] Johannes Köhler, Elisa Andina, Raffaele Soloperto, Matthias A. Müller, and Frank Allgöwer. Linear robust adaptive model predictive control: Computational complexity and conservatism. In *IEEE Conference on Decision and Control*, pages 1383–1388, 2019.
- [20] Wilbur Langson, Ioannis Chrysochoos, SV Raković, and David Q Mayne. Robust model predictive control using tubes. *Automatica*, 40(1):125–133, 2004.
- [21] Matthias Lorenzen, Mark Cannon, and Frank Allgöwer. Robust MPC with recursive model update. *Automatica*, 103:461–471, 2019.
- [22] Xiaonan Lu and Mark Cannon. Robust adaptive tube model predictive control. In *American Control Conference*, pages 3695–3701, 2019.
- [23] Xiaonan Lu and Mark Cannon. Robust adaptive model predictive control with persistent excitation conditions. *Automatica*, 152:110959, 2023.
- [24] David Q Mayne, Saša V Raković, Rolf Findeisen, and Frank Allgöwer. Robust output feedback model predictive control of constrained linear systems. *Automatica*, 42(7):1217–1222, 2006.
- [25] I. Petersen. Quadratic stabilizability of uncertain linear systems: Existence of a nonlinear stabilizing control does not imply existence of a linear stabilizing control. *IEEE Transactions on Automatic Control*, 30(3):291–293, 1985.
- [26] Sasa V Rakovic, Eric C Kerrigan, Konstantinos I Kouramas, and David Q Mayne. Invariant approximations of the minimal robust positively invariant set. *IEEE Transactions on Automatic Control*, 50(3):406–410, 2005.
- [27] Saša V Raković, Basil Kouvaritakis, Rolf Findeisen, and Mark Cannon. Homothetic tube model predictive control. *Automatica*, 48(8):1631–1638, 2012.
- [28] H. Messaoud S. M. Veres and Journal of P. Norton. Limited-complexity model-unfalsifying adaptive tracking-control. *International Journal of Control*, 72(15):1417–1426, 1999.
- [29] András Sasfi, Melanie N Zeilinger, and Johannes Köhler. Robust adaptive MPC using control contraction metrics. *Automatica*, 155:111169, 2023.
- [30] Damianos Tranos, Alessio Russo, and Alexandre Proutiere. Self-tuning tube-based model predictive control. In *American Control Conference*, pages 3626–3632, 2023.